Preparation of rice husk ash silica-hydroxyapatite adsorbent for defluoridation of water: Kinetic and equilibrium studies.

Mupa M.*, Mapfaire E., Machingauta C., Muchanyereyi-Mukaratirwa N.

Bindura University of Science Education, Department of Chemistry, Private Bag 1020, Bindura, Zimbabwe.

Abstract : Silica-hydroxyapatite adsorbent was preparedand tested of its applicability in the defluoridation of water. Rice husk ash from Oryza glaberrina rice was used as a silica source. The adsorbent had a bulk density of 0.12 $g·cm^{-3}$.Studies on the effect of contact time, adsorbent dosage, pH and initial fluoride concentration were performed. A maximum adsorption capacity of 5.53 $mg·g^{-1}$ was achieved at a pH of 5. The data fitted well with the Freundlich adsorption isotherm, confirming a multi-layer diffusion. FTIR spectra of adsorption material confirmed the presence of typical absorption bands. The XRF measurements confirmed the presence of major components, Si, Ca and P. XRD confirmed the presence of calcium hydroxyapatite and about 77 % amorphous silica.
Key words : adsorbent, defluoridation, fluorosis, hydroxyapatite, rice husk ash, silica.

Introduction

Fluoride contamination of drinking water due to natural and human activities has led in some communities to a number of health problems. Contamination of ground waterattributed to fluoride has been due fluoride containing minerals such as fluorspar, fluoroapatite, sallaite and cryolite.[1] These minerals are normally insoluble but favorable conditions of heavy rainfall may trigger dissolution of fluorides which eventually leads to contamination of underground water, wells, boreholes and springs. The WHO recommends a maximum fluoride concentration of 1.5 $mg·L^{-1}$ as beneficial and safe for human consumption. Fluoride concentration below 0.5 $mg·L^{-1}$have been reported to cause dental fluorosis, while concentrations above 1.5 $mg·L^{-1}$ may lead to dental fluorosisand a host of other health problems.[2,3]

A number of defluoridation methods are being developed or improved on to combat the problem of fluorosis. These include defluoridation techniques based on adsorption whereby water contaminated with fluoride is passed through an adsorbent whose surface binds fluoride ions thereby achieving separations,[4,5] electrocoagulation[6,7] and membrane filtration.[8] Adsorption techniques have dominated other techniques and review reports suggests that a wide range of adsorbents can be used in the defluoridation of water.[9,10] Common adsorbents for defluoridation are activated alumina, zeolites, bone char, activated clay and activated carbon based on bio or agro-waste.

In this research article we report the preparation of a silica-hydroxyapatite adsorbent using silica derived from rice husk ash and its application in the defluoridation of drinking water. Pure hydroxyapatite can be used as an adsorbent in defluoridation of water but has poor mechanical properties and hence less suitable for continuous flow processes. Different forms of hydroxyapatite have been tested for defluoridation of water. Areview study on the defluoridation efficiency of different materials reported that for hydroxyapatite derived

adsorbents Al-modified hydroxyapatite (32.57 mg·g^{-1}) and nano-hydroxyapatite derived from phosphogypsum (19.74-40.81 mg·g^{-1}) had high adsorption capacities.[4]

Experimental section

Chemicals

Chemicals used for various experiments were of analytical grade and were used without further purification. Ammonia,acetic acid, HCl and NaOH were purchased from Sky Lab (Pvt.) Ltd. Ca(OH)$_2$ and phosphoric acid were supplied by Sigma-Aldrich.

Sampling

Rice husks removed from indigenous rice seeds harvested from a field in Masvingo area of Zimbabwe were pulverized and leached with 2 M HCl for one hour to remove heavy metals. The leached rice husks were washed thoroughly with distilled water and dried over night at 80 ^{o}C. Dried rice husks were ignited in a muffle furnace at 600 ^{o}C for three hours. The resultant white rice husk ash (RHA) sample was used for the preparation of silica-hydroxyapatite adsorbents.

Preparation of Hydroxyapatite

The synthetic procedure for hydroxyapatite was adapted from the literature.[11]A cloudy suspension of calcium hydroxide was vigorously stirred at 40 ^{o}C for one hour. To the suspension 0.3 M H$_3$PO$_4$ was added dropwise for 50 minutes. The reaction mixture was vigorously stirred overnight. The resultant precipitate was filtered off, washed thoroughly with distilled water before being dried overnight at 110 ^{o}C. The dried product was used for the preparation of various silica-hydroxyapatite composites as described below.

Preparation of Silica-Hydroxyapatite Adsorbent

The method for the preparation of sodium silicate rich solution from Rice husk ash was adapted from a research article.[12]The synthetic procedure for the composite adsorbent is illustrated in Figure 1 below. For an optimized procedure, RHA with 96 % silica by XRF analysis(15 g) was suspended in 50 ml 3 M NaOH and refluxed for 3 hours. After which residues were filtered off. Tothe clear filtrate 5 g hydroxyapatite was added. The reaction mixture was further stirred for another 5 hours after which acetic acid was added until a pH of 5 was attained. The composite was filtered off and washed thoroughly with distilled water before being dried at 120 ^{o}C overnight.
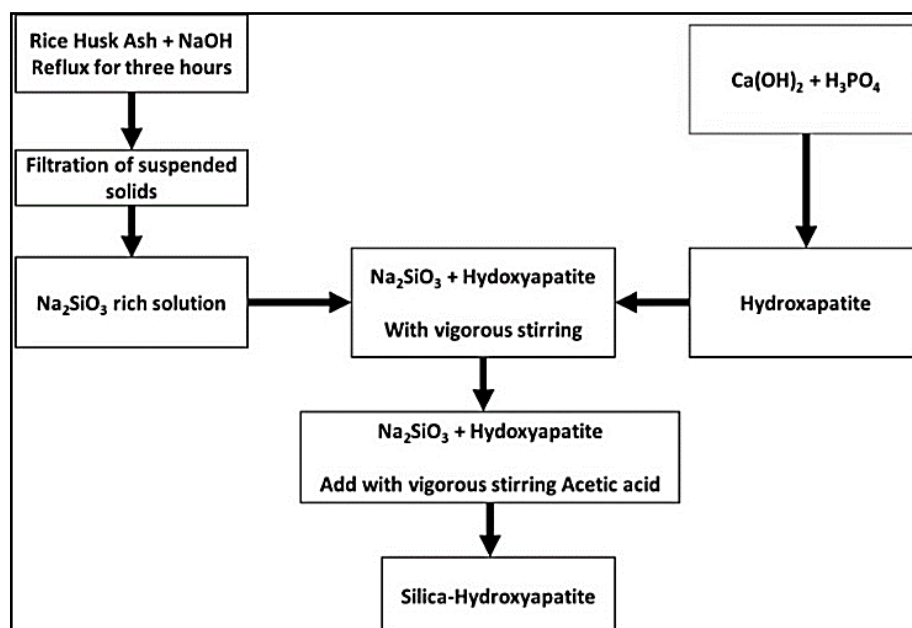

Figure 1: Synthetic steps for Silica-hydroxyapatite adsorbent.

Characterization of Adsorbent

A Thermo Fisher Scientific Nicolet™ iS™5 MIR FTIR spectrophotometer equipped with an ATR accessory and an OMNIC™ software was used record spectra of samples. An Oxford X-Supreme 8000 XRF spectrometer with a tungsten tube X-ray source was used to determine the composition of silica-hydroxyapatite adsorbent. A Bruker D2 Phase XRD with Cu-$K_\alpha$source was used to determine morphology of samples the result is shown on Figure 4. SEM images were recorded on a Jeol JSM 6510 scanning electron microscopeand the results are illustrated on Figure 5.

Batch Adsorption Studies

A 500 ppm stock solution of NaF was prepared and used to prepare 5, 10, 20 ppm synthetic fluoride solutions by serial dilution. Fixed amounts of adsorbent placed in 150 ml plastic bottles were agitated with 50 ml of synthetic fluoride solutions. The suspension was agitated at 25 ^{o}C in a thermostatted bath at 180 rpm for a period of up to 180 minutes. Samples were analyzed using a fluoride ion selective electrode at ten-minute intervals. Adsorption experiments were optimized in terms of pH, contact time, initial fluoride concentration and adsorbent dosage.

The amount of fluoride adsorbed per unit adsorbent was calculated using the following equation:

$$q_t = \frac{(C_0 - C_t)V}{m}$$
(1)

where q_t is the amount of fluoride adsorbed at time t in mg·g^{-1}, C_0 the initial fluoride concentration in mg·L^{-1}, C_t the equilibrium concentration at time t in mg·L^{-1}, V the volume of synthetic fluoride solution and m mass of adsorbent in g.

The removal efficiency was calculated using the following equation:

$$\% - removal = \frac{(C_0 - C_t)}{C_0} \times 100$$
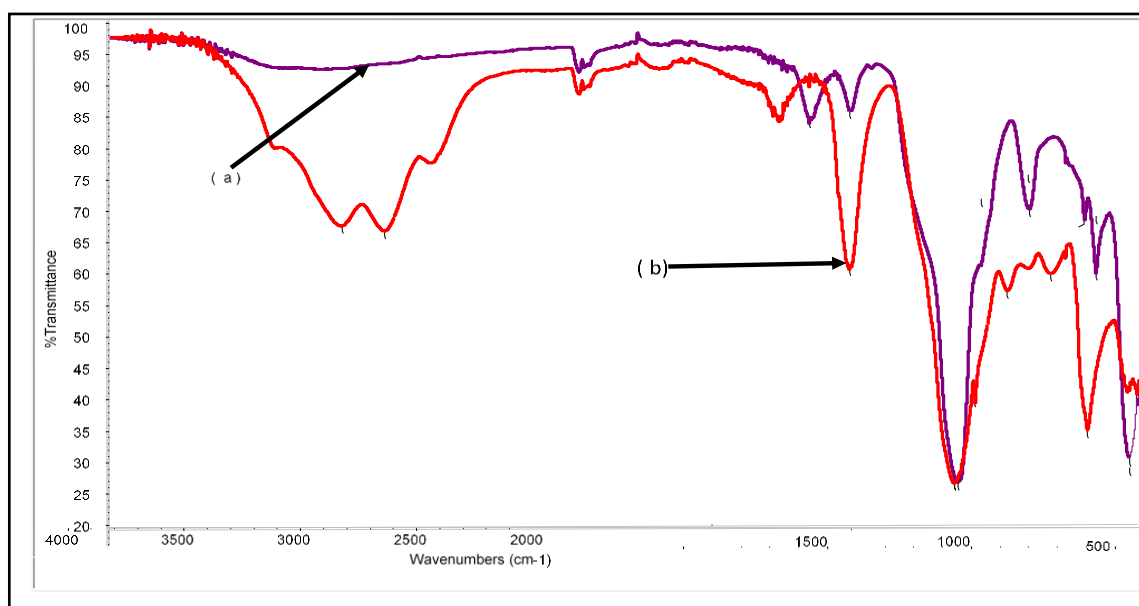(2)

Results and Discussion

Figure 2: FTIR spectra of silica (a)and silica-hydroxyapatite adsorbents (b).

Transmittance FTIR spectra of silica gel and silica gel-hydroxyapatite composites are shown in Figure 1 below. The broad absorption band between3000 and 3500 cm^{-1} can be attributed to -OH groups of the hydroxyapatite and adsorbed water molecules. A strong absorption band at about 1000 cm^{-1} is due to an overlap of Si-O-Si and PO$_4$asymmetric stretching vibrations. A sharp absorption peak around 1480 cm^{-1} can be attributed to –OH bending. Similar absorption bands for silica have been observed by other authors.[13,14]

The results of XRF analysis are shown in Figure 3. The spectrums confirmed the presence of silica (1.739 keV) and P (2.014 keV) and Ca (3.693 keV) in the hydroxyapatitein proportions indicated in the table (insert).
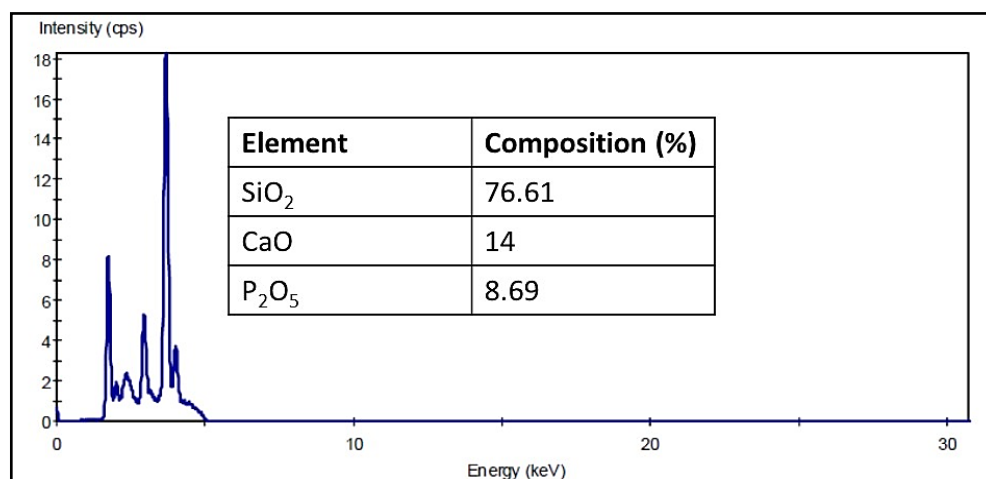

Element	Composition (%)
SiO$_2$	76.61
CaO	14
P$_2$O$_5$	8.69

Figure 3: XRF spectrum of the silica-hydroxyapatite adsorbent.

The XRD pattern for the silica-hydroxyapatite adsorbent is shown on Figure 4. The broad and strong peak at 2θ= 22° is due to 80 % amorphous silica in the adsorbent. A series of strong and sharp peak at 2θ=26° and 2θ=31-35°indicate the presence of crystalline hydroxyapatite. A similar pattern has also been observed in a study on the formation of hydroxyapatite on mesoporous silica gel particles.[15]
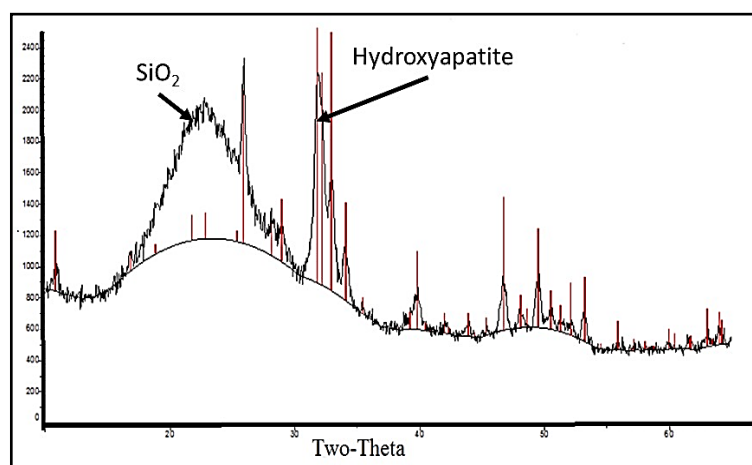

Figure 4: XRD pattern of the silica-hydroxyapatite adsorbents

SEM imagesfor the Silica-hydroxyapatite are shown in Figure 5A and B. The images showed the presence of a crystalline due to hydroxyapatite and amorphous phase due to silica. Optical microscopy images are shown in Figure 5 C and D and clearly show the presence of hydroxyapatite embedded insilica matrix.
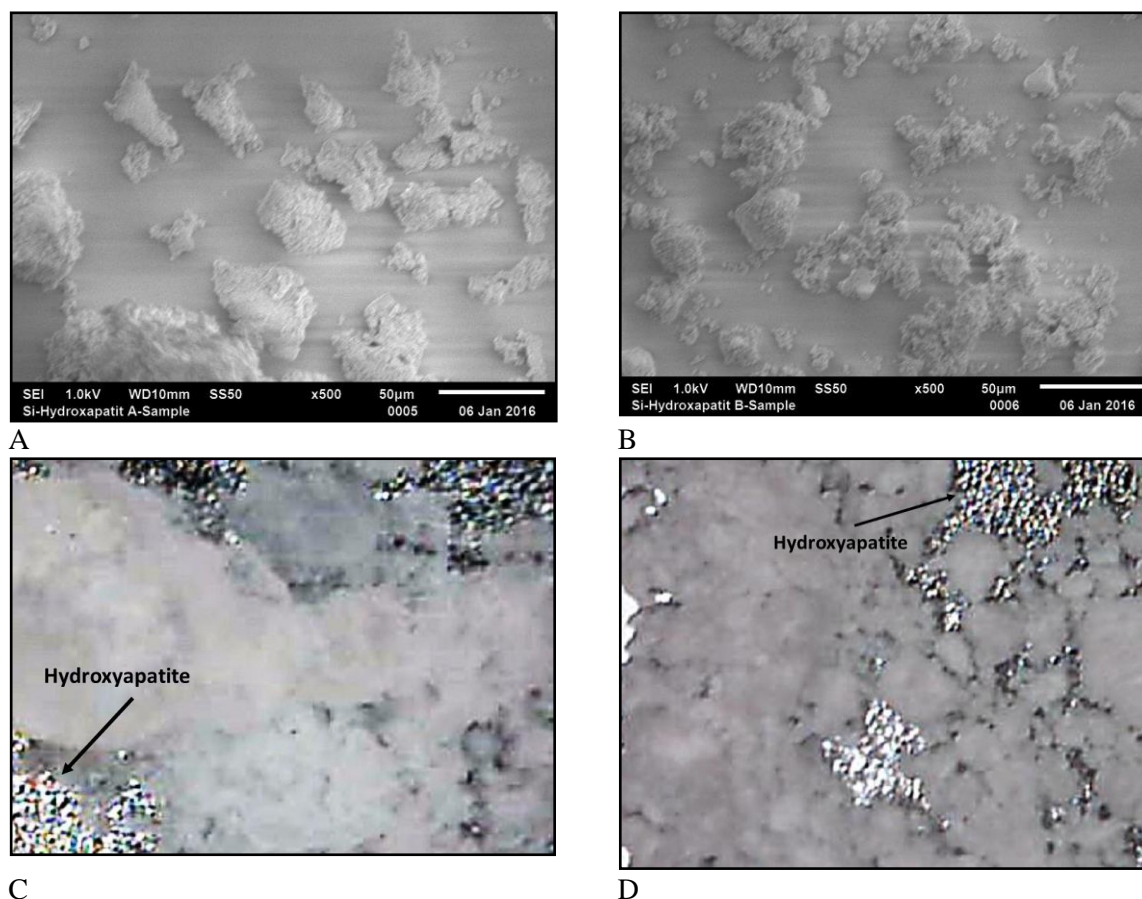
Figure5: SEM images (A and B) and optical microscopy images (C and D) of hydroxyapatite and silica-hydroxyapatite adsorbents.

Adsorption Experiments

Effect of pH

The effect of pH on removal efficiency is illustrated in Figure 6. Optimum fluoride adsorption of 5.42 mg·g^{-1} was achieved at pH5. Above pH5 adsorption capacity decreased drastically. It has been stated that at low pH, the hydroxyl groups of silica-hydroxyapatite composite are protonated making it easier to be replaced by fluoride ions than at higher pH.[16] The suggestion was further supported that the OH- groups represent active sitesresponsible for fluoride uptake in the hydroxyapatite.[17]
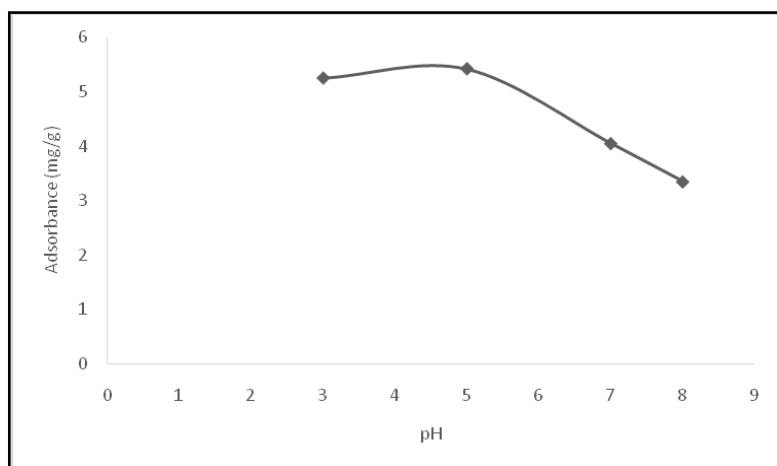

Figure 6: Effect of pH (T = 25 ^{o}C, agitation = 180 rpm, adsorbent dosage = 0.8 g)

Effect of adsorbent dosage

The effect of adsorbent dosage was investigated for the dosage range of 0.1-1.0 g at an optimum pH of 5. The results are illustrated in Figure 7. From the figure it can be seen that a maximum removal efficiency of 70 % was achieved. The removal efficiency is less than what has been reported with pure hydroxyapatite.[16] This can be due to a reduced number of active cites in the composite.
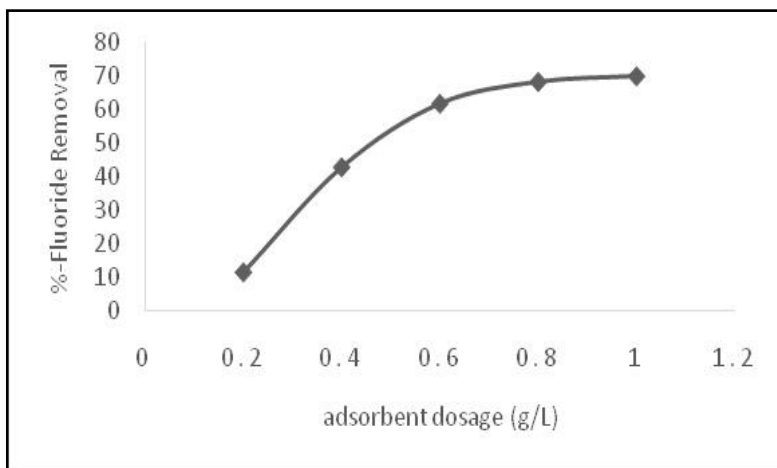

Figure 7: Effect of adsorbent dosage (pH = 5, agitation speed = 180 rpm, T = 25 ^{o}C).

Effect of contact time

The effect of contact time on fluoride ion adsorption was investigated over a period of 50 minutes at an adsorbent dosage of 0.8 g and fluoride concentration of 10 mg·l^{-1}. The result is illustrated in Figure 8. The diagram shows that the equilibrium was reached after 40 minutes. The adsorption can be considered to be rather too slow. In one similar study equilibrium concentration was reached after 30 minutes with synthetic nano-hydroxyapatite. The study concluded that the adsorption process was not by ion exchange mechanism as the equilibrium took much longer to achieve.[16]
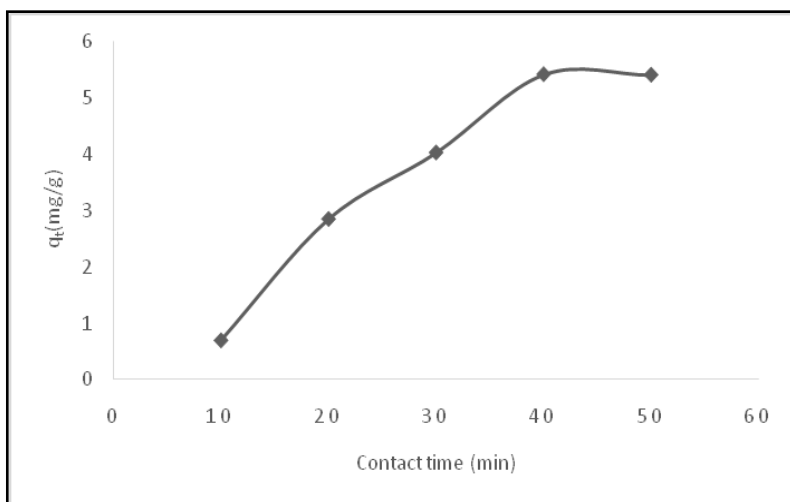

Figure 8: Effect of contact time (pH=5, agitation speed = 180 rpm, adsorbent = 0.8 g)

Adsorption Isotherms

Adsorption isotherm studies were carried out in order to establish the nature of adsorption processes. Data was fitted on to the Langmuir and Freundlichadsorption isotherm models.

The Langmuir model assumes that solute particles form a mono layer at specific and numerous homogeneous sites within the adsorbent surface.[18,19] The adsorption model has ever since its adoption been used to explain a number of adsorption processes. The Langmuir adsorption isotherm is described by the following equation:

$$q_e = \frac{q_m K_L C_e}{1 + K_L C_e} \qquad (4)$$

where q_e is the amount of Fluoride ion adsorbed per unit surface ($mg \cdot g^{-1}$), q_m is the maximum mono layer adsorption capacity in $mg \cdot g^{-1}$, C_e is the equilibrium fluoride concentration ($mg \cdot L^{-1}$), K_L is the Langmuir adsorption constant ($L \cdot mg^{-1}$). The linearized form of the above equation is:

$$\frac{C_e}{q_e} = \frac{1}{K_L q_m} + \frac{1}{q_m} C_e \qquad (5)$$

whereby $\frac{C_e}{q_e}$ is plotted against C_e, and the values of q_m and K_L are determined from the slope and intercept in the graph respectively. Langmuir adsorption isotherm for fluoride removal is illustrated in Figure 9. From the R^2 value of 0.7926, one can conclude that the adsorption data does not fit well in to the Langmuir model. This may be due to the heterogeneity nature of the adsorbent material.
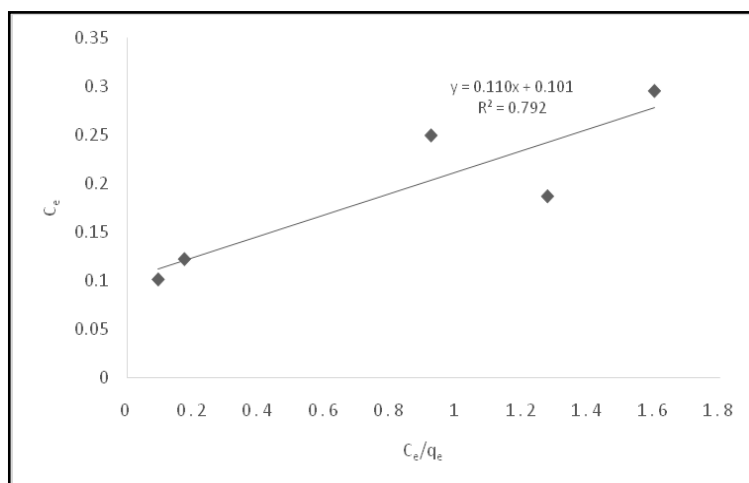

Figure 9: Langmuir adsorption isotherm for fluoride adsorption.

The Freundlich adsorption isotherm assumes that the adsorbate forms a multilayer on heterogeneous surfaces with exponential decrease in the adsorption site energy distribution and is given by the following equation.

$$q_e = K_f C_e^{1/n} \qquad (7)$$

where q_e is the equilibrium adsorption capacity ($mg \cdot g^{-1}$), K_f the Freundlich constant, $1/n$ an empirical constant, and C_e the equilibrium concentration ($mg \cdot L^{-1}$). From equation 7, it can be observed that the Freundlich adsorption is exponential and assumes that as the concentration of the adsorbate increases, the concentration of adsorbate on the adsorbent surface also increases. The linearized form of the above equation is:

$$\log q_e = \log K_f + \frac{1}{n} \log C_e \qquad (8)$$

The plot $\log q_e$ versus $\log C_e$ gives a linear graph. The slope and intercept give the parameters n and K_f respectively.[20] One such plot is shown in Figure 10 below and from the R^2(0.9946) one can conclude that the adsorption data fits well into the Freundlich model.
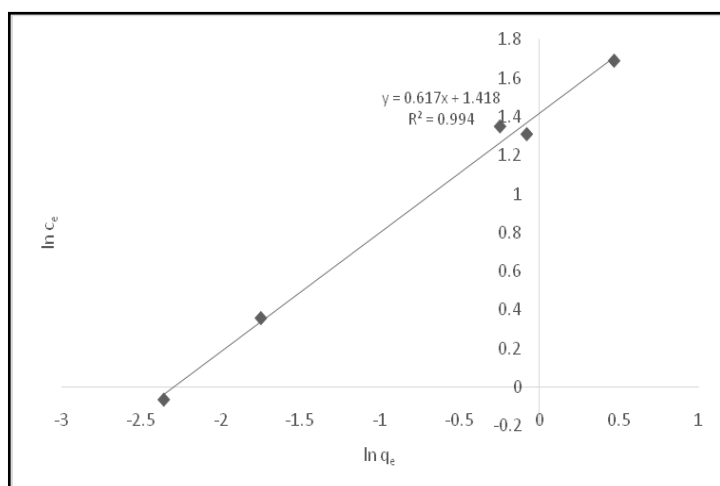
Figure 10: Freundlich isotherm for fluoride adsorption.

Kinetics of Fluoride Adsorption

Kinetic studies were carried out to explain mechanism of fluoride adsorption. Two models, pseudo-first and pseudo second order kinetics were used to study the adsorption mechanism on the silica-hydroxyapatite composite

The pseudo-first order kinetic model is described by the following equation:

$$\frac{dq_t}{dt} = k_1(q_e - q_t)$$
(9)

where q_t is the amount of adsorbed fluoride at time t in $mg \cdot g^{-1}$, q_e the equilibrium adsorption capacity in $mg \cdot g^{-1}$, k_1 the pseudo-first order rate constant in min^{-1} and t the contact time in minutes. The linearized form of this equation described as the Lagergren's equation is:

$$\ln(q_e - q_t) = lnq_e - k_1t$$
(10)

The rate constant k_1 and intercept ln q_e is determined from the graph on $ln(q_e-q_t)$ is determined against t. The results are shown in Figure 11.
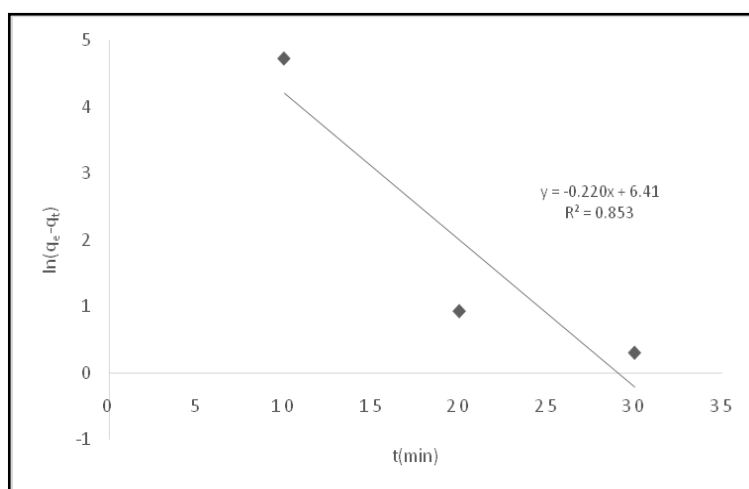

Figure 11: Pseudo-first order plot for fluoride adsorption

The pseudo-second order kinetics for adsorption has the form:

$$\frac{dq_t}{dt} = k_2(q_e - q_t)^2$$

(12)

The linearized form of the equation is:

$$\frac{t}{q_t} = \frac{1}{k_2 q_e^2} + \frac{t}{q_e}$$

(13)

where k_2 is the equilibrium rate constant for the pseudo-second order adsorption in $mg \cdot g^{-1} \cdot min^{-1}$ and the initial adsorption rate h given by $k_2 q_e^2$ in $mg \cdot g^{-1} \cdot min$. A plot of versus t is linear over the whole range. The value of rate constant can be found from the intercept of the curve and q_e is determined from the slope. The result is illustrated in figure 12. Compared to the pseudo-first order plots, there is a higher co-relation of values for the pseudo-second order adsorption process. R^2 values of more than 0.99 have also been obtained for all pseudo-first order plots for the adsorption of fluoride on to hydroxyapatite.[21]
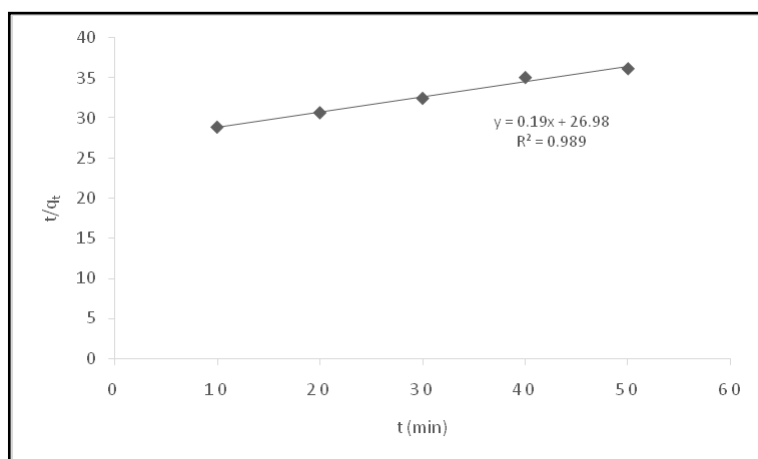

Figure 12: Pseudo-second order plot for fluoride adsorption.

Conclusion

The studydemonstrated the feasibility of preparing of silica-hydroxyapatite adsorbent using RHA as a silica source and apply the adsorbent in the removal of fluoride ions. Adsorption data fitted well with Freundlich adsorption isotherm. The adsorbent was found to have a maximum fluoride adsorption capacity of $5.53 \ mg \cdot g^{-1}$. The mechanism of adsorption was best described by the pseudo-second order kinetic model. FTIR spectra showed the existence of typical IR absorptions bands.

Acknowledgement

References

1. Mohapatra M., Anand S., Mishra B.K., Giles D E and Singh P., Review of fluoride removal from drinking water, J. Environ. Manage2009, 91, 67-77.
2. Tewari A., Dubey A., Defluoridation of drinking water: Efficacy and Need, J. Chem. Pharm. Res. 2009, 1(1), 31-37.
3. Peckham S., Awofeso N., Water Fluoridation: A critical review of the physiological effects of ingested fluoride as a public health intervention,Scientific World J. 2014,Article ID 293019, 10 pages. http://dx.doi.org/10.1155/2014/2014/293019.

4.   Tomar V., Kumar D., A critical study on efficiency of different materials for fluoride removal from aqueous media, Chem. Cent. J. 2013, **7,** 51. http://journal.chemistrycentral.com/content/7/1/51

5.   Fan X., Parker D. J., Smith M. D., Adsorption kinetics of fluoride removal on low cost materials, Water Res. 2003, 37, 4929-4937.

6.   Mameri N., Lounici H., Belhocine D., Grib H., Piron D. L., Yahiat Y., Defluoridation of Sahara water by small plant electrocoagulation using bipolar aluminum electrodes, Sep. Purif. Technol. 2001, 24,113-119.

7.   Essadki A. H., Gourich B., Vial Ch., Delmas H., Bennajah M., Defluoridation of drinking water by electrocoagulation/electrofloatation in a stirred tank reactor with a comparative performance to an external-loop airlift reactor, J. Hazard. Mater. 2009,168(1-3), 1325-1333. Doi:10.1016/J.JHAZMAT.2009.03-021.

8.   Diaye C. K., Moulin P., Domiguez L., Millet J. C., Charbit F., Removal of fluoride from electronic industrial effluent by RO membrane separation, Desalination 2005,173, 28-32.

9.   Surendra R. Dass G., Fluoride contamination in drinking water, Resources and Environment 2013, 3(3),53-58.

10.   Mann S., Mundial A., Performance of low-cost adsorbents for the removal fluoride ions, International Journal of Engineering Science and Innovative Technology 2014, 3(3), 437-443.

11.   Santos M. H., Oliveiria M., Souza L. P. F., Mansur H. S., Vasconcelos W. L., Synthesis Control and characterization of hydroxyapatite by wet precipitation process, Mater. Res. 2004, **7**(4), 625-630.

12.   Kalapathy U., Proctor A., Shultz J., An improved method for production of silica from rice hull ash, Bioresour. Technol. 2002, 85**,** 285-289.

13.   Sarawade P. B., Kim J. K., Park J. K., Kim H. K., Influence of solvent exchange on the physical properties of sodium silicate based aerogel prepared at ambient pressure, Aerosol Air Qual. Res. 2006, 6(1), 93-105.

14.   Riman R. E., Suchanek W. L., Byrappa K., Chen C. W., Shuk P., Oakes C. S., Solution synthesis of hydroxyapatite designer particles, Solid State Ionics 2002, 151, 393-402.

15.   Díaz A., Lopez T., Manjarrez J., Basadella E., Martínez-Blanes J. M., Odriozola J. A., Growth of hydroxyapatite in a biocompatible mesoporous ordered silica, Acta Biomater. 2006, 2,173-179.

16.   Sundaram C. S., Viswanathan N., Meenakshi S., Defluoridation Chemistry of synthetic hydroxyapatite at nano scale: Equilibrium and Kinetic Studies, J. Hazard. Mater. 2008, 155**,** 206-215.

17.   Habuda M., Ravancic M. E., Flanagan A., A review on adsorption of fluoride from aqueous solution, Materials 2014,**7,** 6317-6366. DOI: 10.3390/ma7097317

18.   Langmuir I., The constitution and fundamental properties of solids and Liquids – Part I, J. Am. Chem. Soc. 2018, 40, 1361-1403.

19.   Hamdaoui O. Naffrechouy E., Modelling of adsorption isotherms of phenol and chlorophenol onto granular activated carbon. Part I: Two parameter models and equations allowing determination of thermodynamic parameters, J. Hazard. Mater. 2007, 147, 381-394.

20.   Foo K. Y., Hameed B. H., (2010) Insights into modelling of adsorption isotherm systems, Chem. Eng. J. 2010,**156,** 2-10.

21.   Gao S., Sun R., Wei Z., Zhao H., Li H., Hu F., Size-dependent defluoridation properties of synthetic hydroxyapatite,J. Fluorine Chem.2009, 130, 550-566.

*****

Extra Page not to be Printed out.

For your Research work, for citations/References Log on to=

International Journal of ChemTech Research

International Journal of PharmTech Research

★★★★★